An Adaptive Sliding Mode Controller for Buck Converter in Continuous Conduction Mode

Siew-Chong Tan, Y. M. Lai, Chi K. Tse, and Martin K. H. Cheung
Department of Electronic & Information Engineering
The Hong Kong Polytechnic University
Hong Kong, China
email: ensctan@eie.polyu.edu.hk

***Abstract*— This paper proposes a new adaptive sliding mode controller for buck converter operating in the continuous conduction mode. Through gain scheduling, the controller is designed to monitor the output loading condition, and adaptively changes its control parameters to give optimal dynamic performances corresponding to any loading variations. Simulations have been carried out to verify the idea. The results show faster transient response and reduced steady state error during over-loaded operation, and improved controller's reliability during under-loaded operation, under the adaptive controller.**

I. Introduction

Conventionally, only classical controllers (P, PI, or PID) based on linearized small-signal converter models are employed for the control of power converters [1] – [3]. However, they often fail to perform satisfactorily under large parameter or load variations [4]. Hence, with the objective of attaining good performance under parameter and load variations, sliding mode (SM) controller was introduced to power converters [5] – [10].

However, there is a slight drawback with conventional SM controlled converters, that is, their dynamic and steady state performances deteriorate if the loading condition differs from the nominal condition. When operated below the nominal load, there will be overshoots and ringing during transient. When operated above the nominal load, the response will be slow with a high steady state error. This will be further discussed in section 2.

Therefore, in this paper, an adaptive sliding mode controller which can optimize the dynamic performance of the converter during load variations, is proposed. This is realized through the incorporation of a *gain scheduling scheme* [11] into the conventional SM controller. The scheme automatically varies the controller parameters according to the output loading condition. The investigation was conducted on a commonly used topology: buck converter in continuous conduction mode (CCM). Nevertheless, the idea can be extended to other topologies.

Section II reviews the conventional SM controller for the buck converter. Section III details the proposed adaptive SM controller. Simulation results for both the adaptive and non-adaptive (conventional) SM controlled buck converters are evaluated in section IV. Finally, section V summarizes the findings of the paper.

II. Sliding Mode Controller For Buck Converter

A typical SM controller for switching converters has two control modes: voltage mode and current mode. Here, voltage mode control is employed, i.e. output voltage, $V_{\rm o}$, is the parameter to be controlled.

A. Mathematical Model of Buck Converter

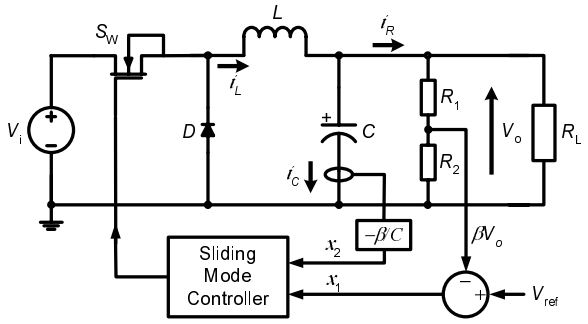

Fig. 1. Sliding mode controlled buck converter.

Fig. 1 shows the schematic diagram of a SM voltage controlled buck converter. Here, the voltage error, x_1, is

$$x_1 = V_{\rm ref} - \beta V_{\rm o} \tag{1}$$

where $V_{\rm ref}$ is the constant reference voltage and $\beta = R_2/(R_1+R_2)$ is the sensing ratio of the output voltage. The rate of change of voltage error, x_2, is

$$x_2 = \dot{x_1} = -\beta\frac{dV_{\rm o}}{dt} = -\beta\frac{i_C}{C} \tag{2}$$

where $i_C = C(dV_{\rm o}/dt)$ is the capacitor current, and C is the capacitance. Since $i_C = i_L - i_R$, where i_L and i_R represent the inductor and load currents respectively, differentiation of eqn. (2) with respect to time gives

$$\dot{x_2} = \frac{\beta}{C}\frac{d(i_R - i_L)}{dt}. \tag{3}$$

Using $i_R = V_{\rm o}/R_{\rm L}$ where $R_{\rm L}$ is the load resistance, and the averaged equation of a CCM inductor current:

$$i_L = \int \frac{uV_{\rm i} - V_{\rm o}}{L}dt \tag{4}$$

where V_i is the input voltage; L is the inductance; and $u = 1$ or 0 is the switching state, we have

$$\begin{aligned} \dot{x_2} &= \frac{\beta}{R_\mathrm{L}C}\frac{dV_\mathrm{o}}{dt} + \frac{\beta}{C}\left(\frac{V_\mathrm{o} - uV_\mathrm{i}}{L}\right) \\ &= -\frac{x_2}{R_\mathrm{L}C} + \frac{V_\mathrm{ref}}{LC} - \frac{x_1}{LC} - u\frac{\beta V_\mathrm{i}}{LC}. \end{aligned} \tag{5}$$

Finally, from (2) and (5), a state space model describing the system is derived as

$$\begin{bmatrix} \dot{x_1} \\ \dot{x_2} \end{bmatrix} = \begin{bmatrix} 0 & 1 \\ -\frac{1}{LC} & -\frac{1}{R_\mathrm{L}C} \end{bmatrix} \begin{bmatrix} x_1 \\ x_2 \end{bmatrix} + \begin{bmatrix} 0 \\ -\frac{\beta V_\mathrm{i}}{LC} \end{bmatrix} u + \begin{bmatrix} 0 \\ \frac{V_\mathrm{ref}}{LC} \end{bmatrix} \tag{6}$$

B. Design of Sliding Mode Voltage Controller

In SM control, the controller employs a sliding surface to decide its input states, u, to the system. For SM voltage controller, the switching states, u, which corresponds the turning on and off of the power converter's switch, is decided by the sliding line [8]:

$$S = \alpha x_1 + x_2 = \boldsymbol{J}\boldsymbol{x} = 0 \tag{7}$$

where α is a positive quantity (stability condition); $\boldsymbol{J}$ = [α, 1]; and $\boldsymbol{x} = [x_1, x_2]^T$. It has been derived in [10] that

$$\alpha = \frac{1}{R_\mathrm{L}C}. \tag{8}$$

Graphically, this is simply a straight line on a $x_1 - x_2$ phase-plane with gradient α (see Fig. 2). However, the implication of α is more than a 'decision maker'. It actually determines the dynamic response of the system in SM with a first order time constant: $\tau = 1/\alpha$. To ensure that a system follows its

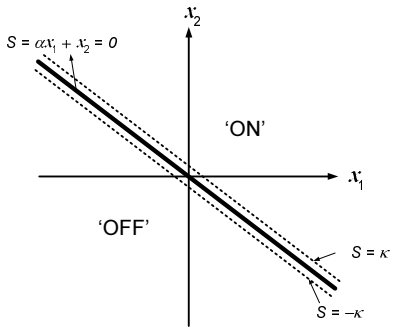

Fig. 2. Sliding line on $x_1 - x_2$ phase-plane.

sliding surface, a control law must be imposed. In our system, the control law is defined as:

$$u = \begin{cases} 1 = \text{'ON'} & \text{when } S > \kappa \\ 0 = \text{'OFF'} & \text{when } S < -\kappa \end{cases} \tag{9}$$

in accordance with the hitting condition [10], that the system trajectories eventually reach the sliding line. The reason for choosing $S > \kappa$ and $S < -\kappa$ as the switching boundary is to introduce an hysteresis band which determines the switching frequency of the converter. If the parameters of the state variables are such that $S > \kappa$, switch S_W of buck converter shown in Fig. 1 will turn on. Conversely, it will turn off when $S < -\kappa$. In the region $-\kappa \leq S \leq \kappa$, S_W remains in its previous state. Thus, this prevents the SM controller from operating at a frequency that is too high for the power switch to respond. Indirectly, it also alleviates the effect of chattering which could induce extremely high frequency switching. The switching conditions are graphically represented in Fig. 2.

Next, to ensure that SM control is realizable in this system, an existence condition [8] must be obeyed:

$$\lim_{s \to 0} S \cdot \dot{S} < 0. \tag{10}$$

Thus, by substituting the time derivative of (7), the condition for SM control to exist is

$$\dot{S} = \begin{cases} \boldsymbol{J}\dot{\boldsymbol{x}} < 0 & \text{for } 0 < \mathrm{S} < \xi \\ \boldsymbol{J}\dot{\boldsymbol{x}} > 0 & \text{for } -\xi < \mathrm{S} < 0 \end{cases} \tag{11}$$

where ξ is an arbitrarily small positive quantity. Substituting (6) and (9) into (11), the inequalities become

$$\begin{aligned} \lambda_1 &= \left(\alpha - \frac{1}{R_\mathrm{L}C}\right)x_2 - \frac{1}{LC}x_1 + \frac{V_\mathrm{ref} - \beta V_\mathrm{i}}{LC} < 0 \\ \lambda_2 &= \left(\alpha - \frac{1}{R_\mathrm{L}C}\right)x_2 - \frac{1}{LC}x_1 + \frac{V_\mathrm{ref}}{LC} > 0 \end{aligned} \tag{12}$$

where

$$\begin{aligned} \lambda_1 &= \boldsymbol{J}\dot{\boldsymbol{x}} \quad \text{for} \quad 0 < S < \xi \\ \lambda_2 &= \boldsymbol{J}\dot{\boldsymbol{x}} \quad \text{for} \quad -\xi < S < 0. \end{aligned} \tag{13}$$

The above conditions are depicted in Fig. 3 for the two respective situations: (a) $\alpha > 1/R_\mathrm{L}C$ and (b) $\alpha < 1/R_\mathrm{L}C$. In both figures, Region 1 represents $\lambda_1 < 0$ and Region 2 represents $\lambda_2 > 0$. SM will only occur on the portion of the sliding line that covers both Regions 1 and 2. In this case, this portion is within A and B, where A is the intersection of $S = 0$ and $\lambda_1 = 0$; and B is the intersection of $S = 0$ and $\lambda_2 = 0$. Since the phase trajectory will slide to the origin only when it touches S within AB, it will overshoot the sliding line if the trajectory landed outside AB (as shown in Fig. 3(a)). This results in an overshoot in the voltage response when $\alpha > 1/R_\mathrm{L}C$.

C. Problem Definition

In the design of the SM controller, α is typically set as a constant parameter corresponding to a nominal operating condition, to facilitate practical implementation. This makes the sliding line static irrespective of the operating condition. Strictly speaking, this is an inappropriate approach, which leads to unsatisfactory performance when there is a large deviation in the operating conditions. This can be further understood from the buck converter example.

From (8), it is known that α is proportional to filter capacitor, C, which is constant, and inversely proportional to load resistance, R_L, which *may not* be constant. Consequently, we can re-express it as:

$$\alpha \propto \frac{1}{R_\mathrm{L}}. \tag{14}$$

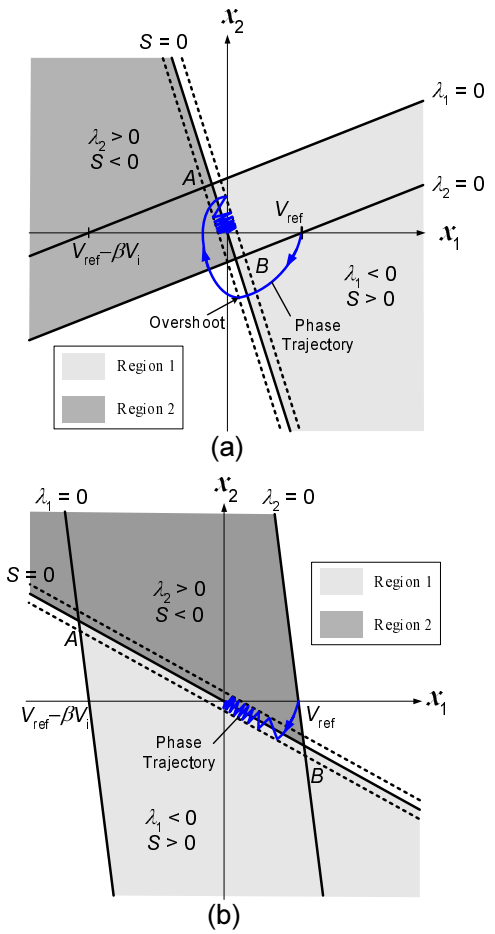

Fig. 3. Regions of existence of SM in phase plane: (a) $\alpha > 1/R_{\rm L}C$ and (b) $\alpha < 1/R_{\rm L}C$.

Now, consider operating the buck converter in an under-loaded condition whereby $R_{\rm L(dy)} > R_{\rm L(nom)}$, the nominal load. This correspondingly gives

$$\alpha_{\rm (dy)} < \alpha_{\rm (nom)} \tag{15}$$

which supposedly results in an angular decrement, θ, in the gradient of the sliding line as shown in Fig. 4, where

$$\theta = \arctan \alpha_{\rm (nom)} - \arctan \alpha_{\rm (dy)}. \tag{16}$$

However, as mentioned earlier, the sliding line is designed to be static with gradient $\alpha_{\rm (nom)}$. Hence, there is a mismatch between the required sliding line and the actual sliding line employed in the system. This results in a reduction of sliding-mode existence region causing overshoots and ringing in the transient response as was discussed in the previous section.

Conversely, when it is operated at an over-loaded condition, $\alpha_{\rm (dy)} > \alpha_{\rm (nom)}$ and $\tau_{\rm (dy)} < \tau_{\rm (nom)}$. If $\alpha_{\rm (nom)}$ is employed, the response of the converter will be slower than it should be. Consequently, the slowness in the response dynamics results in poorer regulation and therefore, a higher steady state error. This can be observed in the simulation results shown later in the paper.

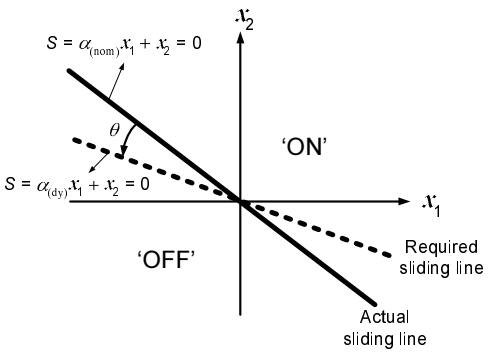

Fig. 4. Sliding line of an under-loaded system.

III. Adaptive Sliding Mode Voltage Controller For Buck Converter

The reason for introducing an adaptive system into the SM voltage controller is to alleviate the problems associated with the deviation of loading conditions. This is possible by manipulating the relationship of α and $R_{\rm L}$ described in (14), which gives

$$\alpha = \frac{R_{\rm L(nom)}}{R_{\rm L}}\alpha_{\rm (nom)} \tag{17}$$

where α is the instantaneous sliding line gradient; $R_{\rm L}$ is the instantaneous loading resistance; and $R_{\rm L(nom)}$ and $\alpha_{\rm (nom)}$ are respectively the nominal loading resistance and sliding line gradient. Since it is not possible to measure resistance directly, the relationship:

$$R_{\rm L} = \frac{V_{\rm o}}{i_{\rm R}} \quad \text{where } i_{\rm R} \neq 0 \tag{18}$$

is exploited to obtain the instantaneous loading resistance. The incorporation of (17) and (18) will result in an adaptive SM controller which will monitor the output voltage and load current, and adjust α accordingly to provide optimal dynamic performances corresponding to any load variation. This can be performed by gain scheduling [11], which effectively generates a value k corresponding to

$$k = \frac{R_{\rm L(nom)}}{R_{\rm L}}. \tag{19}$$

The value of k is then used to vary α in the SM voltage controller through a multiplier, i.e.,

$$\alpha = k\alpha_{\rm (nom)}. \tag{20}$$

A block diagram of the proposed adaptive SM voltage controller is illustrated in Fig. 5. It is worth mentioning that this controller can easily be implemented using low cost op amps and simple analog multiplier/divider ICs.

IV. Simulation Results and Discussion

Preliminary studies of the adaptive SM voltage controller are conducted on the buck converter described in Fig. 1. In order to compare the performance of adaptive and non-adaptive controllers, simulations using a benchmark converter with the specifications given in Table I are carried out in Matlab/Simulink. The simulation step size is 1 μs.

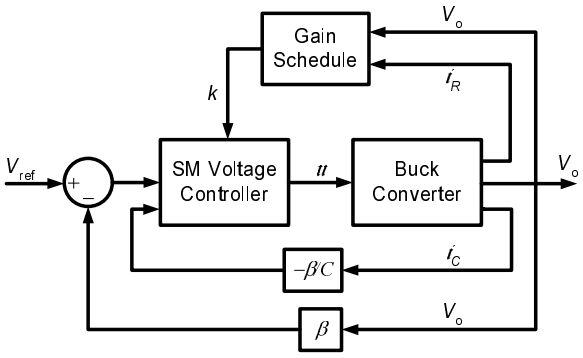

Fig. 5. An adaptive sliding mode controlled buck converter.

TABLE I
SPECIFICATIONS OF BUCK CONVERTER

Description	Parameter	Nominal Value
Input voltage	V_i	48 V
Inductance	L	10 mH
Inductor resistance	r_L	100 mΩ
Capacitance	C	470 μF
Capacitor resistance	r_C	100 mΩ
Load resistance	R_L	4 Ω
Output voltage	V_o	12 V

A. Over-loaded Operation

To demonstrate the effectiveness of the adaptive SM controller in overloaded condition, we start our simulation with a nominal load of 4 Ω, then apply a step load change to 2 Ω at time = 0.02 s. The simulation results are shown in Figs. 6, 7, 8, 9, and 10.

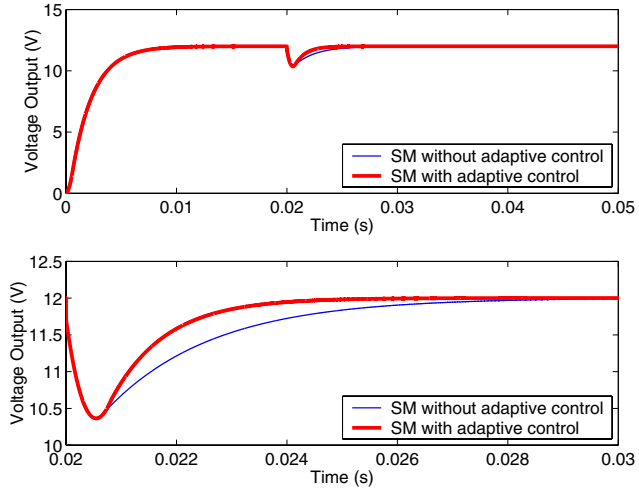

Fig. 6. Output voltage response under step load change from 4 Ω to 2 Ω at time = 0.02 s.

In Fig. 6, it is shown that the voltage drop recovers more quickly with the adaptive controller when the step load change is applied. This is because the non-adaptive controller has slower dynamic response under over-loaded condition due to its sliding line being of lower gradient than the required sliding line. This matches the discussion in section 2.

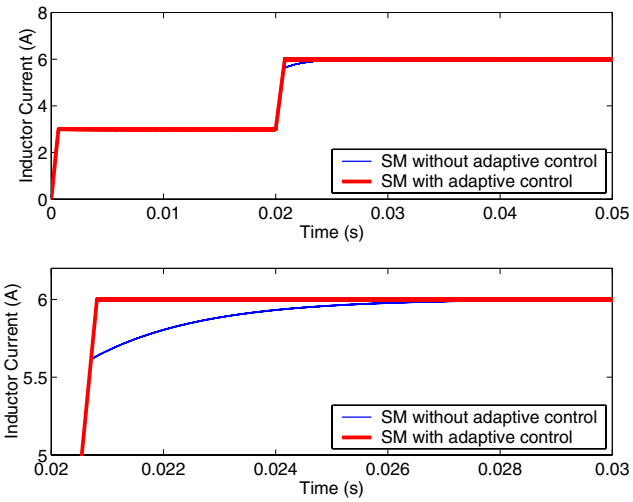

Fig. 7. Inductor current response under step load change from 4 Ω to 2 Ω at time = 0.02 s.

Correspondingly, Fig. 7 shows the inductor current of the adaptive SM controlled converter settling to its steady state at a time of 0.0055 s earlier than the non-adaptive SM controlled converter.

The steady state output voltage waveforms shown in Fig. 8 also matches the theoretical discussion that due to faster dynamic response, and therefore tighter control, the adaptive controlled converter has a lower output voltage error than the non-adaptive controlled converter.

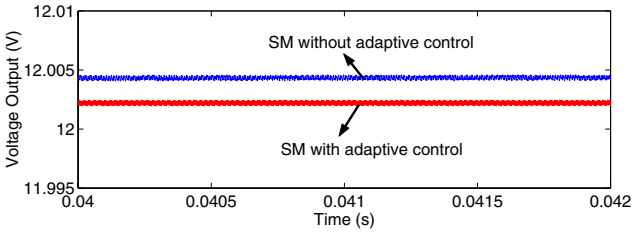

Fig. 8. Steady state output voltage after step load change.

Figs. 9 and 10 show respectively the phase trajectories of the non-adaptive and the adaptive SM operations. For the non-adaptive SM operation, the trajectory moves from point A to B, where it hits the nominal sliding line, $S_{(\mathrm{nom})}$, leading it to settle at origin O. When the load change was applied (time = 0.02 s), the trajectory was dislocated to a new position X. The SM control then moves it to point Y where it once again hits $S_{(\mathrm{nom})}$ leading it back to O. For the adaptive SM operation, the starting trajectory is the same. However, after the change in load, which dislocated the trajectory to X, the trajectory then moves to point Y, which is a different position from that of the non-adaptive phase plot. Here (Fig. 10), Y is a point on the new sliding line, $S_{(\mathrm{dy})}$, which corresponds to the new load, R_{L}. From this position, the trajectory slides to its origin O via $S_{(\mathrm{dy})}$. It should be noted that $S_{(\mathrm{dy})}$ has a steeper gradient than $S_{(\mathrm{nom})}$ since $R_{\mathrm{L}} < R_{\mathrm{L(nom)}}$.

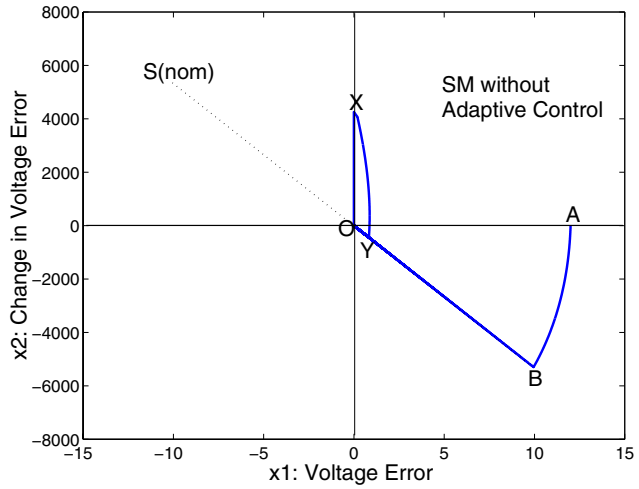

Fig. 9. Phase plane plot under step load change from 4 Ω to 2 Ω for non-adaptive SM control.

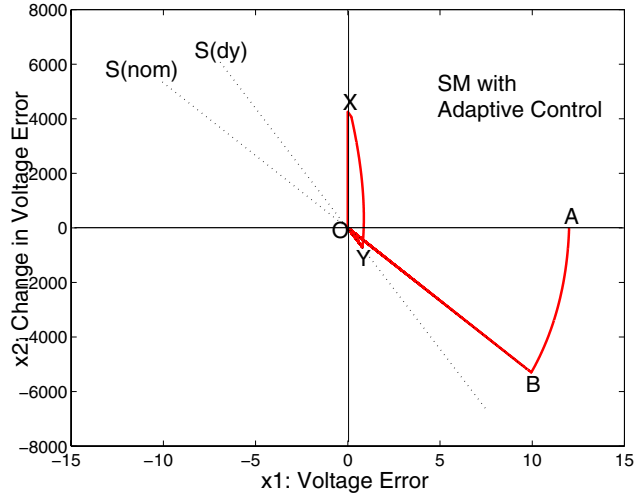

Fig. 10. Phase plane plot under step load change from 4 Ω to 2 Ω for adaptive SM control.

B. Under-loaded Operation

For the under-loaded operation, we start our simulations with a nominal load of 4 Ω, then apply a step load change to 18 Ω at time = 0.02 s.

Fig. 11 shows both the output voltage and inductor current waveforms for the adaptive and non-adaptive operations, and Figs. 12 and 13 show the corresponding phase trajectories. It should be noted that in this case, $S_{(\mathrm{dy})}$ has a lower gradient than $S_{(\mathrm{nom})}$ since $R_{\mathrm{L}} > R_{\mathrm{L(nom)}}$.

Furthermore, it should also be clarified that although the output voltage response of the non-adaptive operation is faster than the adaptive operation, the inductor current waveform shows that it is at the expense of a large current undershoot[1]. This is undesired and may lead to controller failure when the current undershoot is large enough to make the converter enter

[1]In practical circuit, there will also be ringing due to the presence of parasitic components.

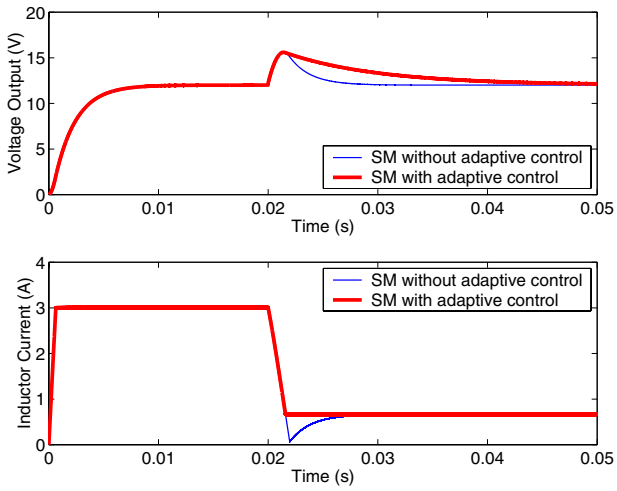

Fig. 11. Output voltage (top) and inductor current (bottom) responses under step load change from 4 Ω to 18 Ω at time = 0.02 s.

the discontinuous conduction mode (DCM). This is because in DCM, state variable x_2 is non-continuous and practically non-measurable. As the SM controller is designed to work only with feedback state variables that are continuous and accessible, a condition that is only possible under CCM, it may lose its control and exhibits unpredictable behavior during DCM. In reliability's viewpoint, the ability of the adaptive controller to maintain the full controllability of the converter through the slowing down of the output voltage transient response, is an important feature. This makes the adaptive controller more reliable than the non-adaptive controller in light-load operations. However, this is not to say that slow dynamic response is encouraged in light-load operations. Instead, it should be ensured that while maintaining controller's functionality, the transient response time should be sufficiently fast to meet the requirement of the load.

Lastly, in the case of starting the non-adaptive SM controller in the under-loaded operation, the fast output voltage dynamic will result in a large inductor current overshoot, which increases the stress of circuit components. Typically, soft-starting and/or over-current protection circuits is required to be incorporated for fault protection in the non-adaptive SM controller. However, with the ability to adjust the sliding gradient to eliminate ringing and overshoots, such circuits are not necessary in the adaptive SM controller.

V. Conclusion

The proposed adaptive SM controller alleviates the problem of deteriorated dynamic and steady state performances faced by conventional non-adaptive SM controlled buck converter. This is performed by employing the gain scheduling scheme which monitors the output voltage and load current to vary the sliding line of the system. Simulation results showed that the adaptive SM controlled converter has faster dynamic response with reduced steady state error when it is operated above the nominal load, and it eliminates overshoots and ringing in the transient response when operated below the nominal load.

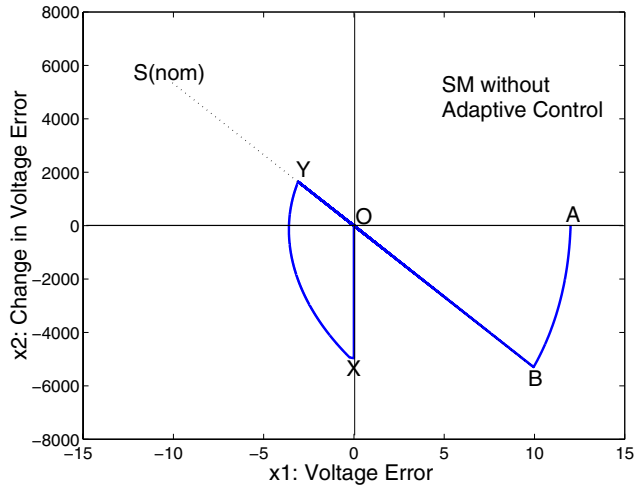

Fig. 12. Phase plane plot under step load change from 4 Ω to 18 Ω for non-adaptive SM control.

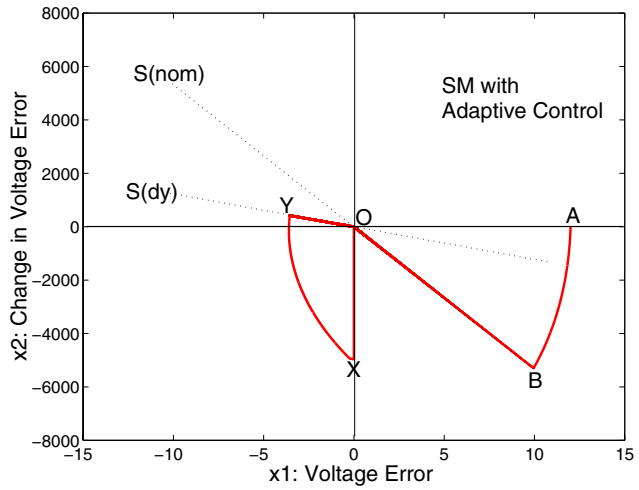

Fig. 13. Phase plane plot under step load change from 4 Ω to 18 Ω for adaptive SM control.

ACKNOWLEDGMENT

The work described in this paper was supported by a grant provided by The Hong Kong Polytechnic University (Project No. G-T379).

REFERENCES

[1] D.M. Mitchell, *DC-DC Switching Regulator Analysis*. New York: McGraw Hill, 1998.

[2] A.J. Forsyth and S.V. Mollow, "Modelling and control of DC-DC converters," *IEE Power Engineering Journal*, vol. 12 no. 5, pp. 229–236, Oct 1998.

[3] J.G. Kassakian, M.F. Schlecht, and G.C. Verghese, *Principles of Power Electronics*. Reading, Mass.: Addison-Wesley, June 1992.

[4] V.S.C. Raviraj and P.C. Sen, "Comparative study of proportional-integral, sliding mode, and fuzzy logic controllers for power converters," *IEEE Transactions on Industry Applications*, vol. 33 no. 2, pp. 518–524, March/April 1997.

[5] J. Mahdavi, M.R. Nasiri, and A. Agah, "Application of neural networks and state space averaging to a DC/DC pwm converter in sliding mode operation," in *Proceedings, IEEE Conference on Industrial Electronics, Control and Instrumentations (IECON)*, vol. 1, pp. 172–177, Oct 2000.

[6] E. Fossas and D. Biel, "A sliding mode approach to robust generation on DC-to-DC nonlinear converters," in *Proceedings, IEEE International Workshop on Variable Structure Systems*, pp. 67–71, Dec 1996.

[7] C. Morel, J.-C Guignard, and M. Guillet, "Sliding mode control of DC-to-DC power converters," in *Proceedings, 9th International Conference on Electronics, Circuits and Systems*, vol. 3, pp. 971–974, Sep. 2002.

[8] V. Utkin, J. Guldner, and J.X. Shi , *Sliding Mode Control in Electromechanical Systems*. London, U.K.: Taylor and Francis, 1999.

[9] E. Fossas and A. Pas, "Second order sliding mode control of a buck converter," in *Proceedings, The 41st IEEE Conference on Decision and Control*, vol. 1, pp. 346–347, Dec. 2002.

[10] G. Spiazzi and P. Mattavelli, "Sliding-mode control of switched-mode power supplies," Ch. 8, *The Power Electronics Handbook*. Boca Raton FL: CRC Press LLC, 2002.

[11] K.J. Astrom and B. Wittenmark, *Adaptive Control*. Reading, Mass.: Addison-Wesley, 2nd ed., 1995.